Naval Research Laboratory

Washington, DC 20375-5320

Remote Atmospheric Lasing

PHILLIP SPRANGLE
JOSEPH PEÑANO

Beam Physics Branch
Plasma Physics Division

BAHMAN HAFIZI

Icarus Research, Inc.
Bethesda, Maryland

DANIEL GORDON

Beam Physics Branch
Plasma Physics Division

MARLAN SCULLY

Texas A&M University
College Station, Texas

Princeton University
Princeton, New Jersey

September 24, 2010

REPORT DOCUMENTATION PAGE

Form Approved
OMB No. 0704-0188

1. REPORT DATE (DD-MM-YYYY) 24-09-2010	2. REPORT TYPE Interim	3. DATES COVERED (From - To) July 2010 – August 2010

4. TITLE AND SUBTITLE

Remote Atmospheric Lasing

5a. CONTRACT NUMBER

5b. GRANT NUMBER

5c. PROGRAM ELEMENT NUMBER
67-9466-00

6. AUTHOR(S)

Phillip Sprangle, Joseph Peñano, Bahman Hafizi,* Daniel Gordon, and Marlan Scully†

5d. PROJECT NUMBER

5e. TASK NUMBER

5f. WORK UNIT NUMBER

7. PERFORMING ORGANIZATION NAME(S) AND ADDRESS(ES)

Naval Research Laboratory
4555 Overlook Avenue, SW
Washington, DC 20375-5320

8. PERFORMING ORGANIZATION REPORT NUMBER

NRL/MR/6790--10-9284

9. SPONSORING / MONITORING AGENCY NAME(S) AND ADDRESS(ES)

Office of Naval Research
One Liberty Center
875 North Randolph St. Suite 1425
Arlington, VA 22203-1995

10. SPONSOR / MONITOR'S ACRONYM(S)

ONR

11. SPONSOR / MONITOR'S REPORT NUMBER(S)

12. DISTRIBUTION / AVAILABILITY STATEMENT

Approved for public release; distribution is unlimited.

13. SUPPLEMENTARY NOTES

*Icarus Research, Inc., P.O. Box 30780, Bethesda, MD 20824-0780
†Department of Physics and Electrical Engineering, Texas A&M University, College Station, TX 77843/Departments of Chemistry and Aerospace & Mechanical Engineering, Princeton University, Princeton, NJ 08544

14. ABSTRACT

This paper considers a remote atmospheric lasing configuration which utilizes a combination of an ultrashort pulse laser to form a plasma filament (seed electrons) by tunneling ionization and a heater beam which thermalizes the seed electrons. The thermalized electrons collisionally excite the nitrogen molecules and induce lasing in the ultraviolet. The lasing gain is sufficently high to reach saturation within the length of the plasma filament. A remotely generated ultraviolet source may have applications for standoff detection of biological and chemical agents.

15. SUBJECT TERMS

Nitrogen laser   UV sources
Atmospheric lasing   Chem/bio detection

16. SECURITY CLASSIFICATION OF:			17. LIMITATION OF ABSTRACT	18. NUMBER OF PAGES	19a. NAME OF RESPONSIBLE PERSON Phillip Sprangle
a. REPORT Unclassified	b. ABSTRACT Unclassified	c. THIS PAGE Unclassified	UL	11	19b. TELEPHONE NUMBER (include area code) (202) 767-3493

Standard Form 298 (Rev. 8-98)
Prescribed by ANSI Std. Z39.18

Remote Atmospheric Lasing

Phillip Sprangle[1], Joseph Peñano[1], Bahman Hafizi[2], Daniel Gordon[1] and Marlan Scully[3,4]

[1]*Plasma Physics Division, Naval Research Laboratory, Washington DC 20375*
[2]*Icarus Research, Inc, PO Box 30780, Bethesda, MD 20824-0780*
[3]*Departments of Physics and Electrical Engineering,*
Texas A&M University, College Station, TX 77843
[4]*Departments of Chemistry and Aerospace & Mechanical Engineering,*
Princeton University, Princeton, NJ 08544

Abstract

We propose and analyze a remote atmospheric lasing configuration which utilizes a combination of an ultrashort pulse laser to form a plasma filament (seed electrons) by tunneling ionization and a heater pulse which thermalizes the seed electrons. Electrons collisionally excite nitrogen molecules and induce lasing in the ultraviolet. The lasing gain is sufficiently high to reach saturation within the length of the plasma filament. A remotely generated ultraviolet source may have applications for standoff detection of biological and chemical agents.

The atmospheric propagation of ultrashort pulse lasers (USPLs) having ~ TW power levels and pulse durations of ~ 100 fsec are strongly affected by various interrelated processes [1,2]. These include diffraction, Kerr focusing, group velocity dispersion, spectral broadening, self phase modulation, photo-ionization, plasma defocusing, and pulse energy depletion. An intense laser pulse propagating in air can be longitudinally and transversely focused at remote distances (> km) and reach intensities sufficient to ionize the air. Longitudinal pulse compression is achieved by introducing a negative frequency chirp on the pulse while nonlinear transverse focusing is caused by the Kerr effect [1-4]. As a result the laser intensity is enhanced (> 10^{13} W/cm^2), resulting in ionization and a plasma filament ~ 1 m in length, ~ 100 μm in radius, and electron density of $N_e \sim 10^{16}$ cm^{-3} [2].

1

A remote UV generation scenario has recently been proposed in which air molecules are Raman or two-photon pumped to the appropriate excited state [5,6]. In this scheme, molecular excitations are achieved via simultaneous action of two synchronized picosecond laser pulses with a frequency difference or sum which is resonant with a transition. In another publication, backscattered fluorescence from N_2 molecules and ions has been observed in experiments in which a USPL-generated plasma filament was optically pumped [7].

We propose and analyze a remote atmospheric lasing configuration based on collisionally exciting the N_2 lasing line at $\lambda = 337\,nm$ in a heated plasma filament, as illustrated in Fig. 1. A secondary heater pulse is used to maintain and thermalize the electrons. Thermal electrons of a few eV can induce a population inversion in N_2 leading to the vibrational-electronic transition $C^3\Pi_u \rightarrow B^3\Pi_g$ at 337 nm. Nitrogen lasers are typically based on collisional excitation using electrical discharges [8-10]. In the present configuration the UV radiation is generated in both the forward and backward directions along a filament with a gain sufficiently high to reach saturation. For a $1\mu m$ wavelength heater beam the Kerr nonlinearity can be the source of third harmonic generation and a seed for lasing at 337 nm.

The density matrix and Maxwell equations [11,12] together with the electron heating and ionization equations are solved. The N_2 lasing model consists of an open two level system denoted by levels 3 (upper) and 2 (lower) respectively. Since levels 3 and 2 are weakly excited the population of level 1 (ground) is taken to be fixed. The population of the excited levels are given by

$$\partial N_3 / \partial \tau = v_{CE,13} N + v_{CE,23} N_2 - v_3 N_3 - v_{stim} (N_3 - N_2), \tag{1a}$$

$$\partial N_2 / \partial \tau = v_{CE,12} N + (v_{CD,32} + \Gamma_{32}) N_3 - v_2 N_2 + v_{stim} (N_3 - N_2), \tag{1b}$$

where $\tau = t - z/c$, z is the position within the filament, t is time, and c is the speed of light. N_n, are densities of the nth level, $N \approx N_1 = 0.8 N_a$ is the ground state density, $N_a = 2.7 \times 10^{19}\,cm^{-3}$ is the air density, $v_3 = v_{CD,31} + v_{CD,32} + \Gamma_{31} + \Gamma_{32}$ is the decay rate of level 3, $v_2 = v_{CD,21} + v_{CE,23} + \Gamma_{21}$ is the decay rate of level 2, Γ_{ij} is the radiative (spontaneous) decay from level i to j, $v_{CE,ij}$ is the collisional excitation rate from level i to j, and $v_{CD,ij}$ is the collisional de-excitation rate from level i to j ($i, j = 1, 2, 3$), $v_{stim} = \sigma_{stim} I / \hbar \omega$ is the stimulated emission rate, I is the UV laser intensity, ω is the lasing frequency,

$\sigma_{stim} = (3\lambda^2/4\pi)(\Gamma_{32}/\gamma_{23})\gamma_{23}^2/(\Delta\omega_{32}^2 + \gamma_{23}^2)$ is the stimulated emission cross section,

$\Gamma_{32} = (4/3)(\omega/c)^3|\mu_{32}|^2/\hbar$, μ_{32} is the dipole moment between levels 3 and 2,

$\gamma_{23} = \gamma_{23}^{(col)} + (1/2)(v_2 + v_3)$ is the dipole decay rate, and $\gamma_{23}^{(col)}$ is the dipole dephasing rate due to

collisions (no population transfer). The dephasing rate $\gamma_{23}^{(col)}$ is the dominant contribution to γ_{23}.

The lasing intensity is given by

$$(\partial/\partial z + \Gamma_d)I = \varepsilon I_{stim}/(c\tau_{rad,32}) + \sigma_{stim}\Delta N I, \tag{2}$$

where Γ_d is the spatial damping rate, ε is a geometric filling factor associated with the seed

radiation within the plasma filament, $I_{stim} = \hbar\omega c N_3$, $\tau_{rad,32}$ is the radiative lifetime from level 3

to 2 including the effects of collisions, and $\Delta N = N_3 - N_2$.

For the parameters under consideration a steady state population inversion is difficult to

achieve. However, a transient population inversion can be achieved if $v_{CE,13} > v_{CE,12}$. For a

constant heater pulse amplitude, the population inversion, for $N_3(0) = N_2(0) = 0$, is shown to be

$$\Delta N(\tau) = N(v_{CE13} - v_{CE12})(1 - \tau/\tau_{in})\tau, \qquad (0 < \tau < \tau_{in}) \tag{3}$$

where $\tau_{in} = 2(v_{CE,13} - v_{CE,12})/(v_{CE,13}(v_3 + v_{CD,32} + \Gamma_{32}) - v_{CE,12}(v_2 + v_{CE,23}))$ is typically

$< 1\,\text{nsec}$ and for $T_e = 2\,\text{eV}$ and $N_e = 10^{16}\,\text{cm}^{-3}$, the rates are $v_{CE13} \approx 2\times10^5\,\text{sec}^{-1}$ and

$v_{CE12} \approx 10^5\,\text{sec}^{-1}$.

The collisional excitation rates are dominated by electron excitations while the de-

excitation rates are dominated by molecular collisions. The excitation rate is

$v_{CE,ij} = N_e\langle\sigma_{CE,ij}(v)v\rangle$ where $\sigma_{CE,ij}$ denotes the excitation cross section from level i to j [13] and

$\langle\rangle$ denotes an average over the electron Maxwellian distribution at temperature T_e. The life

times $\tau_3 = 1/v_3$ and $\tau_2 = 1/v_2$ are determined by both spontaneous emission and molecular

collisions but are dominated by molecular collisions. Electron de-excitation contributions to the

life times are negligible. In addition, since level 2 is a metastable state, $\Gamma_{32} \gg \Gamma_{31}$. The

lifetimes of the upper and lower levels are given by [14, 15],

$\tau_3 \approx (\Gamma_{32} + 2.2\times10^6 P[\text{torr}])^{-1} = 0.6\,\text{nsec}$ and $\tau_2 \approx (\Gamma_{21} + 1.9\times10^5 P[\text{torr}])^{-1} = 7\,\text{nsec}$, where

$1/\Gamma_{32} = 38\,\text{nsec}$, $1/\Gamma_{21} = 9\,\mu\text{sec}$ and P is the pressure. The radiative decay time $\tau_{rad,32}$ includes

3

both spontaneous and collisionally induced radiative transitions but is dominated by molecular collisions, i.e., $\tau_{rad,32} \sim \tau_3$. We take $\gamma_{23}^{(col)}$ to be $\sim 10\nu_m$, where $\nu_m \sim 10^{10}\,\text{sec}^{-1}$ is the molecular collision frequency in air. Using the above parameters the stimulated emission cross section is $\sigma_{stim} \approx 10^{-14}\,\text{cm}^2$.

The electron temperature is given by

$$(3/2)\frac{\partial(N_e T_e)}{\partial \tau} = \langle \mathbf{J}\cdot\mathbf{E}_o\rangle - Q_c N_a N_e (1 - T_v/T_e), \tag{4a}$$

$$(3/2)N_a \frac{\partial T_v}{\partial \tau} = Q_c N_a N_e (1 - T_v/T_e), \tag{4b}$$

where $\langle \mathbf{J}\cdot\mathbf{E}_o\rangle$ is the ohmic heating, Q_c is the cooling rate due to all inelastic collisions and T_v is the N_2 vibrational temperature. The cooling rate Q_c includes internal excitation of vibrational, rotational and electronic states of air. At low energies the dominant inelastic cooling process is the excitation of vibrational states of N_2. The cooling rate is obtained from the CHMAIR code [16,17] and can be modeled by $Q_c \approx 3.5\times10^{-8}\exp(-5/(3T_e)) + 6.2\times10^{-11}\exp(-1/(3T_e))$ [18], where $T_e < 2\,\text{eV}$, Q_c is in units of $\text{eV cm}^3/\text{sec}$, and T_e is in units of eV.

The ohmic heating rate is $\langle \mathbf{J}\cdot\mathbf{E}_o\rangle = (\omega_p^2/8\pi)E_{eff}^2/\nu_e$, where $\omega_p = (4\pi q^2 N_e/m)^{1/2}$ is the plasma frequency, $\nu_e = \nu_{en} + \nu_{ei}$ is the electron collision frequency which is the sum of the electron-neutral, $\nu_{en}[\text{sec}^{-1}] \approx 10^{-7}N_a[cm^{-3}]T_e^{1/2}[\text{eV}]$ and electron-ion, $\nu_{ei}[\text{sec}^{-1}] \approx 10^{-5}N_e[cm^{-3}]T_e^{-3/2}[\text{eV}]$ contributions, $E_{eff} = (\nu_e/\omega_o)/(1 + \nu_e^2/\omega_o^2)^{1/2}E_o$ is the effective electric field, E_o is the field amplitude of the heater beam, $I_o = c|E_o|^2/8\pi$ is the heater intensity, and ω_o is the frequency.

The electron density is given by

$$\partial N_e/\partial \tau = \nu_{ion}N_e - \beta N_+ N_e - \eta N_e, \tag{5a}$$

$$\partial N_-/\partial \tau = \eta N_e - \beta_{-+}N_- N_+, \tag{5b}$$

where ν_{ion} is the collisional ionization rate, β is the electron-ion recombination rate, β_{-+} is the ion recombination rate, η is the attachment coefficient, N_- is the negative ion density and $N_+ = N_e + N_-$.

4

The collisional ionization rate is $v_{ion} = v_{ion}(N_2) + v_{ion}(O_2)$ where

$$v_{ion}(X) = v_X (T_e/U_X)^{3/2}(U_X/T_e + 2)\exp(-U_X/T_e) \text{ [19], } X = (N_2, O_2), U_{N_2} = 15.6 \text{ eV},$$

$U_{O_2} = 12.1$ eV, $v_{N_2} = 7.6 \times 10^{11}$ sec^{-1} and $v_{O_2} = 10^{11}$ sec^{-1}.

The dissociative recombination coefficient [18] is $\beta[cm^3/sec] \approx 1.5 \times 10^{-8} T_e^{-0.7}$ for

$T_e < 0.1 eV$ and $\beta[cm^3/sec] \approx 2 \times 10^{-8} T_e^{-0.56}$ for $T_e > 0.1 eV$. The attachment rate [18] is

$\eta[sec^{-1}] = \alpha_2 N_a + \alpha_3 N_a^2$, where $\alpha_2[cm^3/sec] = 2.75 \times 10^{-10} T_e^{-0.5} \exp(-5/T_e)$ and

$\alpha_3[cm^6/sec] = 1.5 \times 10^{-32} T_e^{-1} \exp(-0.052/T_e)$. Typical values for air [18,20] at STP are

$\beta \sim 3 \times 10^{-8}$ cm^3 sec^{-1}, $\beta_{-+} \sim 2 \times 10^{-6}$ cm^3 sec^{-1} and $\eta \sim 10^8$ sec^{-1}.

From Eq. (2), the lasing intensity in the transient regime is

$$I(z,\tau) = \frac{\varepsilon}{c\tau_{rad,32}} \frac{I_{stim}}{(\Gamma_G(\tau) - \Gamma_d)}(\exp((\Gamma_G(\tau) - \Gamma_d)z - 1), \tag{6}$$

where $\Gamma_G(\tau) = \sigma_{stim} \Delta N(\tau)$ is the spatial growth rate and $\Delta N(\tau)$ is given by Eq. (3).

Atmospheric lasing is simulated by solving Eqs. (1), (2), (4), and (5) using a heating

pulse with intensity profile $I_{heater}(z,t) = I_o \sin^2(\pi\tau/\tau_o)$, $0 \le \tau \le \tau_o$, and wavelength $\lambda_o = 1\mu m$.

Ionization by the USPL is assumed to have created a filament with a uniform density,

$N_e(0) = 10^{16}$ cm^{-3} at $T_e(0) = 0.025 eV$. We hold the fluence of the heater pulse constant, i.e.,

$I_o\tau_o = 285$ J/cm^2, vary the pulse duration, and observe the growth of the UV radiation along the

filament. The geometric factor is $\varepsilon \sim (r_f/2L_G)^2$, where $r_f \sim 100\mu m$ is the filament radius,

$L_G = 1/\Gamma_G$ is the gain length, and $\Gamma_d = 0$.

Figure 2(a) plots the UV fluence as a function of position along the filament for heater

pulses with $\tau_o = 0.3, 0.4,$ and 0.5 nsec. Initially there is exponential growth, which is followed

by linear growth as the population inversion is modified by the UV radiation. Figure 2(b) plots

the gain length of the fluence as a function of position. The gain length during the exponential

gain regime is dependent on the heater pulse intensity, i.e., $L_G \approx 0.5, 1,$ and 1.5 mm for

$\tau_o = 0.3, 0.4,$ and 0.5 nsec, respectively. The gain lengths are in good agreement with those

used in Eq. (6). Exponential gain ends after $\sim 13 L_G$ in all three cases.

5

Figure 3 plots the temporal profile of the UV radiation and population inversion at various positions along the filament. In Fig. (3), the heating pulse duration is $\tau_o = 0.4$ nsec, the heater intensity is $I_o = 7 \times 10^{11}$ W/cm^2, and the duration of the initial ΔN is in good agreement with Eq. (3). Figure 3 shows a ~ 0.1 nsec UV pulse forming near the back of the inversion region. As the UV pulse grows ΔN is depleted and the peak of the UV pulse moves forward relative to the heater pulse. After ~ 2 cm of propagation, the peak UV intensity is ~ 8 MW/cm^2 and the fluence is ~ 0.5 mJ/cm^2.

We have analyzed a lasing scheme that can produce UV in the atmosphere at kilometer distances. Other molecular transitions may also be excited and result in lasing, e.g., N_2^+ and O_2. Non-uniformity of the plasma filament may also affect the gain and saturation length [21].

References

[1] P. Sprangle, J. R. Peñano, and B. Hafizi, "Propagation of Intense Short Laser Pulses in the Atmosphere," Phys. Rev. E **66**, 046418 (2002).

[2] A. Couairon and A. Mysyrowicz, Phys. Reports **441**, 47 (2007).

[3] J.R. Peñano, P. Sprangle, B. Hafizi, A. Ting, D.F. Gordon, and C.A. Kapetanakos, Phys. Plasmas **11**, 2865 (2004).

[4] A. Ting, I. Alexeev, D. Gordon, E. Briscoe, J. Penano, R. Fischer, R. Hubbard, P. Sprangle and G. Rubel, "Remote atmospheric breakdown for standoff detection by using an intense short laser pulse," Applied Optics, **44**, 5315 (2005).

[5] V. Kocharovsky, S. Caemron, K. Lehmann, R. Lucht, R. Miles, Y. Rostovtsev, W. Warren, G.R. Welch and M.O. Scully, Proc. Nat. Acad. Sci. **102**, 7806 (2005).

[6] M.O. Scully (private communication).

[7] Q. Luo, W. Liu and S.L. Chin, Appl. Phys. B **76**, 337 (2003).

[8] E.T. Gerry, Appl. Phys. Lett. **7**, 6 (1965).

[9] A.W. Ali, A.C. Kolb and A.D. Anderson, Appl. Opt. **6**, 2115 (1967).

[10] R.T. Brown, J. Appl. Phys. **46**, 4767 (1975).

[11] P.W. Milonni and J.H. Eberly, *Lasers*, Wiley & Sons, New York, NY, 1988.

[12] R.W. Boyd, *Nonlinear Optics*, 3rd edition, Academic Press, Burlington, MA, 2008.

[13] T. Tabata, *et al.*, Atom. Dat. Nucl. Tab. **92**, 3 (2006).

[14] F. Valk, M.Aints, P. Paris, T. Plank, J. Maksimov and A. Tamm, J. Phys. D: Appl. Phys. **43**, 385202, (2010).

[15] H. Umemoto, Phys. Chem. **5**, 5392-5398 (2003).

[16] A.W. Ali, "Electron Energy Loss Rates in Air," NRL Memorandum Report 5400 (1984).

[17] R.F. Fernsler, A.W. Ali, J.R. Greig and I.M. Vitkovitsky, "The NRL CHMAIR Code: A Disturbed Sea Level Air Chemistry Code," NRL Memorandum Report 4110 (1979).

[18] R. Fernsler (Private communication).

[19] Ya. B. Zel'dovich and Yu. P. Raizer, *Physics of Shock Waves and High-Temperature Hydrodynamic Phenomena* (Dover, Mineola, NY, 2002).

[20] Richard Miles (Private communications).

[21] S. Eisenmann, J.R. Peñano, P. Sprangle, and A. Zigler, Phys. Rev. Lett. **100**, 155003 (2008)].
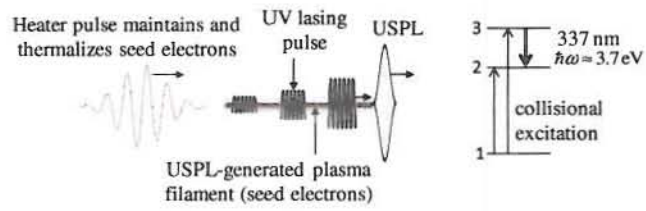
Figure 1: Schematic diagram of remote lasing configuration. An ultrashort pulse laser creates a plasma filament of seed electrons that is heated by a secondary heater pulse. In the energy level diagram for N_2 (right), the energetic electrons collisionally excite the N_2 molecules and induce lasing.
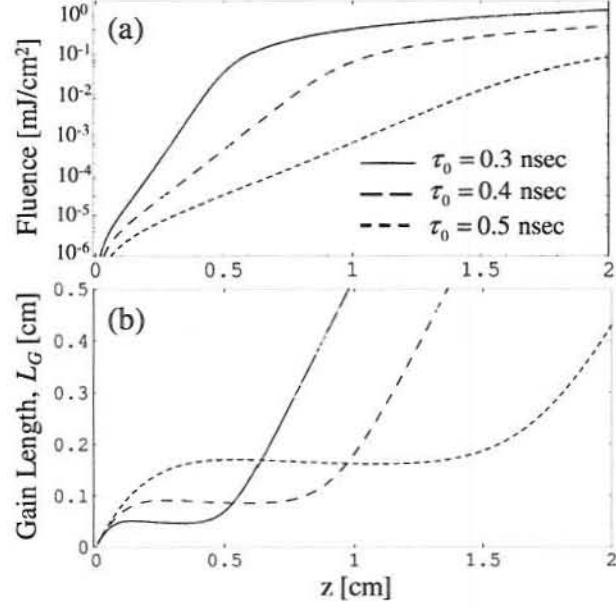
Figure 2: (a) UV fluence as a function of propagation distance, z, for heating pulses with $\lambda_o = 1 \mu m$, $I_o \tau_o = 285 \, J/cm^2$ and pulse durations $\tau_o = 0.3$, 0.4, and 0.5 nsec. (b) Fluence gain length, L_G, as a function of z, corresponding to panel (a).
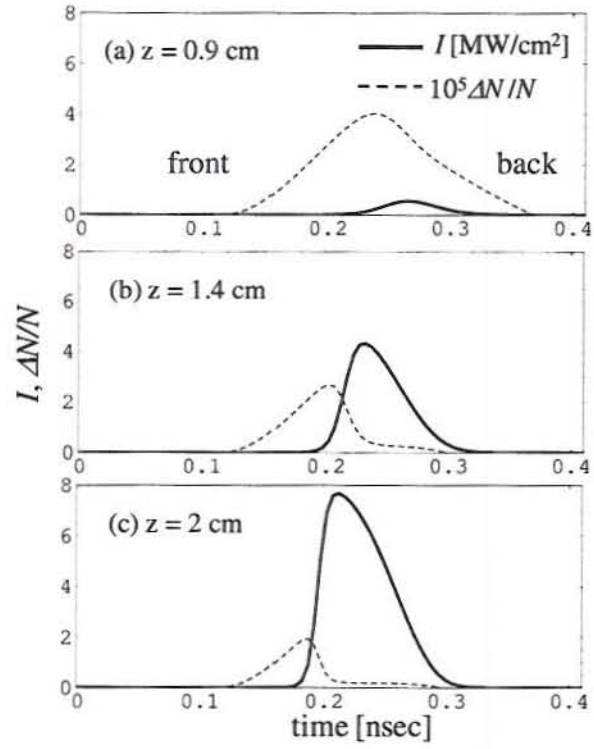
Figure 3: UV intensity, I (solid curves) and normalized population inversion $\Delta N / N = (N_3 - N_2)/N$ (dashed curves) as functions of time at (a) $z = 0.9\,\mathrm{cm}$, (b) $z = 1.4\,\mathrm{cm}$, and (c) $z = 2\,\mathrm{cm}$, for a heating pulse with $\lambda_o = 1\,\mu m$, $I_o \tau_o = 285\,\mathrm{J/cm^2}$ and pulse duration $\tau_o = 0.4\,\mathrm{nsec}$